International Journal on
"Technical and Physical Problems of Engineering"
(IJTPE)
Published by International Organization of IOTPE

ISSN 2077-3528
IJTPE Journal
www.iotpe.com
ijtpe@iotpe.com

September 2012	Issue 12	Volume 4	Number 3	Pages 167-176

A FLEXIBLE NEURAL CONTROLLER FOR TRANSMISSION SYSTEMS EQUIPPED WITH UPFC

A. Hashemi [1]   N.M. Tabatabaei [2]   N. Taheri [3]   S. Naderi [1]

1. Sama Technical and Vocational Training College, Islamic Azad University, Kermanshah Branch, Kermanshah, Iran, ahmad.hashemi.v@gmail.com
2. Electrical Engineering Department, Seraj Higher Education Institute, Tabriz, Iran, n.m.tabatabaei@gmail.com
3. Electrical Engineering Department, Quchan Branch, Islamic Azad University, Quchan, Iran n.taheri.1362@gmail.com

Abstract- Unified power flow controller (UPFC) is the most reliable device in the FACTS concept. It has the ability to adjust all three control parameters effective in power flow and voltage stability. This paper presents the establishment of a linearized Phillips-Heffron model of a power system installed with UPFC to damp low frequency oscillations in a weakly connected system. UPFC has four control loops that, by adding an extra signal to one of them, increases dynamic stability and load angle oscillations are damped. In this paper, after open loop eigenvalue (electro mechanical mode) calculations, state-space equations has been used to design damping controllers and it has been considered to influence active and reactive power flow durations as the input of damping controllers, in addition to the common speed duration of synchronous generators as input damper signals. The potential of UPFC supplementary controllers to enhance the dynamic stability is evaluated based on this model. On the other hands dynamic equations for a power system are nonlinear. To control a nonlinear system, nonlinear controllers are used. Theses controllers are designed based on system state space equations to obtain controlling signal. In this paper a proposed neural controller is used to product a supplementary controlling signal for stabilizing and oscillation damping to overcome the drawbacks of conventional lead-lag controllers in system nonlinear model. The presented control scheme not only performs damping oscillations but also the voltage and power flow control can be achieved. Simulation results carried by Matlab, show the proposed strategy has fast dynamic response.

Keywords: UPFC, Nonlinear Modeling, Neural Controller.

I. INTRODUCTION

As power demand grows rapidly and expansion in transmission and generation is restricted with the limited availability of resources and the strict environmental constraints, power systems are today much more loaded than before. This causes the power systems to be operated near their stability limits [1]. Power system stabilizers (PSSs) aid in maintaining power system stability and improving dynamic performance by providing a supplementary signal to the excitation system [2].

However, PSSs may adversely affect voltage profile, may result in leading power factor, and may not be able to suppress oscillations resulting from severe disturbances, especially those three-phase faults which may occur at the generator terminals [1]. The availability of Flexible AC Transmission System (FACTS) controllers, such as Static Var Compensators (SVC), Thyristor Control Series Compensators (TCSC), Static Synchronous Compensators (STATCOM), and Unified Power Flow Controller (UPFC), has led their use to damping oscillations [3-5].

Extremely fast control action associated with FACTS device operations, they have been very promising candidates for utilization in power system damping enhancement. It has been observed that utilizing a feedback supplementary control, in addition to the FACTS device primary control, can considerably improve system damping and can also improve system voltage profile, which is advantageous over PSSs [1]. Unified power flow controller (UPFC) is the most reliable device in the FACTS concept. It has the ability to adjust all three control parameters effective in power flow and voltage stability. In this paper, a linearized model of a power system installed with a UPFC has been presented.

UPFC has four control loops that, by adding an extra signal to one of them, increases dynamic stability and load angle oscillations are damped. In this paper, after open loop eigenvalue (electro mechanical mode) calculations, state-space equations has been used to design damping controllers and it has been considered to influence active and reactive power flow durations as the input of damping controllers, in addition to the common speed duration of synchronous generators as input damper signals.

Since neural networks have the advantages of high computation speed, generalization and learning ability, they have been successfully applied to the identification and control of nonlinear systems. In [13], a neural controller is used to regulate parameters of a classic PSS. In [14-16], two neural network are have been used to design a power system stabilizer. One of this network is used as a identifier and other one treats as a controller.

In this paper a novel approach is presented to model Heffron-Phillips UPFC systems. In addition to the state-space representation, a block diagram representation is formed to analyze the system stability characteristics. By this modeling approach, it is possible to analyze the small-signal stability of the system and low-frequency oscillation phenomena with the synchronous machine represented by models of varying degrees of detail and the UPFC link in different control modes.

II. PROPOSED POWER SYSTEM INSTALLED WITH UPFC

Figure 1 shows a single-machine-infinite-bus (SMIB) system installed with UPFC. The static excitation system model type IEEE-ST1A has been considered. The UPFC considered here is assumed to be based on pulse width modulation (PWM) converters. The UPFC is a combination of a static synchronous compensator (STATCOM) and a static synchronous series compensator (SSSC) which are coupled via a common dc link, to allow bi-directional flow of real power between the series output terminals of the SSSC and the shunt output terminals of the STATCOM, and are controlled real and reactive series line compensations without an external electric energy source.

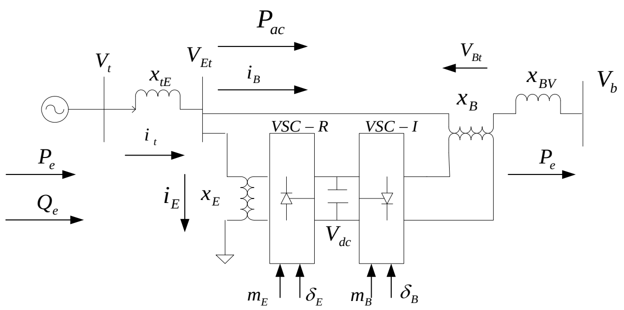

Figure 1. UPFC installed in a SMIB system

The UPFC, by means of angularly unconstraint series voltage injection, is able to control, concurrently or selectively, the transmission line voltage, impendence and angle or alternatively, the real and reactive power flow in the line. The UPFC may also provide independently controllable shunt reactive compensation.

Viewing the operation of the UPFC from the stand point of conventional power transmission based on reactive shunt compensation, series compensation and phase shifting, the UPFC can fulfill all these functions and thereby meet multiple control objectives by adding the injected voltage V_{Bt} with appropriate amplitude and phase angle, to the terminal voltage V_{Et}.

A. Power System Modeling

If the general pulse width modulation (PWM) is adopted for GTO-based VSCs, the three-phase dynamic differential equations of the UPFC are [6]:

$$\Delta\dot{\delta} = \omega_b \Delta\omega$$

$$\Delta\dot{\omega} = \frac{\Delta P_m - \Delta P_e - D\Delta\omega}{M}$$

$$\Delta\dot{E}'_q = \frac{-\Delta E_q + \Delta E_{fd} + (x_d - x'_d)\Delta i_d}{T'_{do}} \tag{1}$$

$$\Delta\dot{E}_{fd} = \frac{-\Delta E_{fd} + K_A(\Delta V_{ref} - \Delta v + \Delta u_{pss})}{T_A}$$

$$\Delta\dot{V}_{dc} = K_7\Delta\delta + K_8\Delta E'_q - K_9\Delta V_{dc} + $$
$$+K_{ce}\Delta m_E + K_{c\delta e}\Delta\delta_E + K_{cb}\Delta m_B + K_{c\delta b}\Delta\delta_B$$

The equations below can be obtained with a line arising from Equation (1).

$$\Delta P_e = K_1\Delta\delta + K_2\Delta E'_q + K_{qd}\Delta V_{dc} + $$
$$+K_{qe}\Delta m_E + K_{q\delta e}\Delta\delta_E + K_{qb}\Delta m_B + K_{q\delta b}\Delta\delta_B \tag{2}$$

$$\Delta E'_q = K_4\Delta\delta + K_3\Delta E'_q + K_{qd}\Delta V_{dc} + $$
$$+K_{qe}\Delta m_E + K_{q\delta e}\Delta\delta_E + K_{qb}\Delta m_B + K_{q\delta b}\Delta\delta_B \tag{3}$$

$$\Delta V_t = K_5\Delta\delta + K_6\Delta E'_q + K_{vd}\Delta V_{dc} + $$
$$+K_{ve}\Delta m_E + K_{v\delta e}\Delta\delta_E + K_{vb}\Delta m_B + K_{v\delta b}\Delta\delta_B \tag{4}$$

$$\Delta V_{dc} = K_7\Delta\delta + K_8\Delta E'_q - K_9\Delta V_{dc} + $$
$$+K_{ce}\Delta m_E + K_{c\delta e}\Delta\delta_E + K_{cb}\Delta m_B + K_{c\delta b}\Delta\delta_B \tag{5}$$

The state-space equations of the system can be calculated by combination of Equations (2) to (5) with Equation (1):

$$\dot{x} = Ax + Bu$$

$$x = [\Delta\delta, \Delta\omega, \Delta E'_q, \Delta E_{fd}, \Delta V_{dc}]^T \tag{6}$$

$$u = [\Delta u_{pss}, \Delta m_E, \Delta\delta_E, \Delta m_B, \Delta\delta_B]^T$$

$$A = \begin{bmatrix} 0 & \omega_b & 0 & 0 & 0 \\ -\frac{K_1}{M} & -\frac{D}{M} & -\frac{K_2}{M} & 0 & -\frac{K_{pd}}{M} \\ -\frac{K_4}{M} & 0 & -\frac{K_3}{T'_{do}} & \frac{1}{T'_{do}} & -\frac{K_{qd}}{T'_{do}} \\ -\frac{K_A K_5}{T_A} & 0 & -\frac{K_A K_6}{T_A} & -\frac{1}{T_A} & -\frac{K_A K_{pd}}{T_A} \\ K_7 & 0 & K_8 & 0 & -K_9 \end{bmatrix} \tag{7}$$

$$B = \begin{bmatrix} 0 & 0 & 0 & 0 & 0 \\ 0 & -\frac{K_{pe}}{M} & -\frac{K_{p\delta e}}{M} & -\frac{K_{pb}}{M} & -\frac{K_{p\delta b}}{M} \\ 0 & -\frac{K_{qe}}{T'_{do}} & -\frac{K_{q\delta e}}{T'_{do}} & -\frac{K_{qb}}{T'_{do}} & -\frac{K_{q\delta b}}{T'_{do}} \\ \frac{K_A}{T_A} & -\frac{K_A K_{ve}}{T_A} & -\frac{K_A K_{v\delta e}}{T_A} & -\frac{K_A K_{vb}}{T_A} & -\frac{K_A K_{v\delta b}}{T_A} \\ 0 & K_{ce} & K_{c\delta e} & K_{cb} & K_{c\delta b} \end{bmatrix}$$

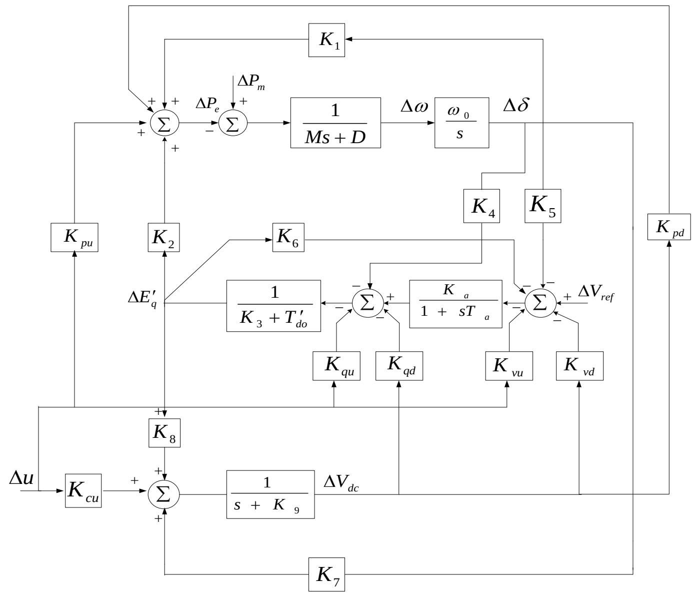

Figure 2. Modified Heffron-Phillips model of SMIB system with UPFC

The Δm_E, Δm_B, $\Delta\delta_E$ and $\Delta\delta_B$ are a linearization of the input control signal of the UPFC and the equations related to the K parameters have been presented in Appendix C. The linearized dynamic model of Equations (2) to (5) can be seen in Figure 2, where there is only one input control signal for *u*. Figure 2 includes the UPFC relating the pertinent variables of electric torque, speed, angle, terminal voltage, field voltage, flux linkages, UPFC control parameters and dc link voltage.

B. Operating Points Calculating in Steady Condition

The primary d-q based axis of voltage, current and load angle of the system, necessary for K parameters calculating in Equation (7), have been obtained for the three conditions shown in Table 1.

- Step 1: First, by solving the four equations below, we compute the parameters V_{td}, V_{tq}, i_{td} and i_{tq} at every operating condition.

$$V_{td}^{\ 2}+V_{tq}^{\ 2}=1 \tag{8}$$

$$V_{td}i_{td}+V_{tq}i_{tq}=P_e \tag{9}$$

$$V_{td}i_{tq}-V_{tq}i_{td}=Q_e \tag{10}$$

$$V_{td}=x_q i_{tq} \tag{11}$$

- Step 2: By solving the 10 equations below, parameters V_{Etd}, V_{Etq}, V_{bd}, V_{bq}, i_{Bd}, i_{Bq}, V_{Btd}, V_{Btq}, i_{Ed} and i_{Eq} will be obtained:

$$\begin{aligned}
&V_{bd}^{\ 2}+V_{bq}^{\ 2}=1\\
&V_{Etd}i_{Bd}+V_{Etq}i_{Bq}=P_{ac}\\
&V_{Etd}=-(x_B+x_{BV})i_{Bq}-V_{Bd}+V_{bd}\\
&V_{Etq}=(x_B+x_{BV})i_{Bd}-V_{Bq}+V_{bq}\\
&V_{Bd}i_{Bd}+V_{Bq}i_{Bq}=P_{dc}\\
&V_{Ed}=V_{Etd}+x_E i_{Eq}\\
&V_{Eq}=V_{Etq}-x_E i_{Ed}
\end{aligned} \tag{12}$$

C. Reactive Power Deviation Signal Modeling

In this section, the dynamic equations relevant to the reactive power deviations will be calculated for use as the input damping control signal. According to Figure 1, the following equations can be written:

$$Q_e=V_{td}i_{tq}-V_{tq}i_{td} \tag{13}$$

$$V_{tq}=E'_q-x'_d i_{td} \tag{14}$$

$$V_{td}=x_q i_{tq} \tag{15}$$

$$Q_e=(x_q i_{tq})i_{tq}-(E'_q-x'_d i_{td})i_{td} \tag{16}$$

Dynamic d-q based equations of currents relevant to the reference system can be obtained as follows:

$$\begin{aligned}
i_{Ed}&=\frac{X_{BB}}{X_{d\Sigma}}E'_q-\frac{m_E\sin\delta_E V_{dc}X_{Bd}}{2X_{d\Sigma}}+\\
&+\frac{X_{dE}}{X_{d\Sigma}}(V_b\cos\delta+\frac{m_B\sin\delta_B V_{dc}}{2})
\end{aligned} \tag{17}$$

$$\begin{aligned}
i_{Eq}&=\frac{m_E\cos\delta_E V_{dc}X_{Bq}}{2X_{q\Sigma}}-\\
&-\frac{X_{qE}}{X_{q\Sigma}}(V_b\sin\delta+\frac{m_B\cos\delta_B V_{dc}}{2})
\end{aligned} \tag{18}$$

$$\begin{aligned}
i_{Bd}&=-\frac{X_{dt}}{X_{d\Sigma}}(V_b\cos\delta+\frac{m_B\sin\delta_B V_{dc}}{2}).\\
&.\frac{X_{dE}}{X_{d\Sigma}}\frac{m_E\sin\delta_E V_{dc}}{2}+\frac{X_E}{X_{d\Sigma}}E'_q
\end{aligned} \tag{19}$$

$$\begin{aligned}
i_{Bq}&=-\frac{m_E\cos\delta_E V_{dc}X_{qE}}{2X_{q\Sigma}}-\\
&-\frac{X_{qt}}{X_{q\Sigma}}(V_b\sin\delta+\frac{m_B\cos\delta_B V_{dc}}{2})
\end{aligned} \tag{20}$$

ΔQ_e signal can be assumed as Equation (21):

$$\begin{aligned}
\Delta Q_e&=K_{10}\Delta\delta+K_{11}\Delta E'_q+K_{12}\Delta V_{dc}+K_{13}\Delta m_E+\\
&+K_{14}\Delta\delta_E+K_{15}\Delta m_B+K_{16}\Delta\delta_B
\end{aligned} \tag{21}$$

From Equations (16) to (20) in comparison with Equation (21) the *K*-constant values can be calculated as shown below:

$$K_{10} = (-2x_q L)(x_{qE} + x_{qt})V_b \cos\delta / (x_{q\Sigma}) + \\ +E'_q V_b \sin\delta((x_{dE} - x_{dt}) / x_{d\Sigma})(2x'_d S + 1) \quad (22)$$

$$K_{11} = ((x_{BB} - x_E) / x_{d\Sigma})(2x'_d S - E'_q) - S \quad (23)$$

$$K_{12} = 2X_q L((x_{Bq} - x_{qE})\cos\delta_E m_E / 2x_{q\Sigma} + \\ +(x_{qt} - x_{qE})\cos\delta_B m_B / 2x_{q\Sigma}) + \\ +(2x'_d L - E'_q)((x_{dE} - x_{Bd})\sin\delta_E m_E / 2x_{d\Sigma} + \\ +(x_{dE} - x_{dt})\sin\delta_B m_B / 2x_{d\Sigma}) \quad (24)$$

$$K_{13} = 2x_q L x_{Bq} - x_{qE})\cos\delta_E V_{dc} / 2x_{q\Sigma} + \\ +(2x'_d S - E'_q)((x_{dE} - x_{Bd})\sin\delta_E V_{dc} / 2x_{d\Sigma}) \quad (25)$$

$$K_{14} = 2x_q L(x_{Bq} + x_{qE})\sin\delta_E V_{dc} m_E / 2x_{q\Sigma} + \\ +(2x'_d S - E'_q)((x_{dE} - x_{Bd})\cos\delta_E m_E V_{dc} / 2x_{d\Sigma}) \quad (26)$$

$$K_{15} = 2x_q L(x_{qt} - x_{qE})\cos\delta_B V_{dc} / 2x_{q\Sigma} + \\ +(2x'_d S - E'_q)((x_{dE} - x_{dt})\sin\delta_B V_{dc} / 2x_{d\Sigma}) \quad (27)$$

$$K_{16} = 2X_q L(x_{qE} - x_{qt})\sin\delta_B V_{dc} m_B / 2x_{q\Sigma} + \\ +(2x'_d S - E'_q)((x_{dE} - x_{dt})\cos\delta_B V_{dc} m_B / 2x_{d\Sigma}) \quad (28)$$

$$L = (m_E \cos\delta_E V_{dc} x_{Bq}) / (2x_{q\Sigma}) - \\ -(x_{qE} / x_{q\Sigma})(0.5 m_B i \cos\delta_B Vdc + V_b \sin\delta) - \\ -(m_E \cos\delta_E Vdc x_{qE}) / (2x_{q\Sigma}) + \\ +(x_{qt} / x_{q\Sigma})(0.5 m_B \cos\delta_B V_{dc} + V_b \sin\delta) \quad (29)$$

$$S = (x_{BB} E'_q / x_{d\Sigma}) - (m_E \sin(\delta_E) V_{dc} x_{Bd}) / (2x_{d\Sigma}) + \\ +(x_{dE} / x_{d\Sigma})(V_b \cos\delta + \\ +0.5 m_B \sin(\delta_B) V_{dc}) - (x_E E'_q / x_{d\Sigma}) + \\ +(x_{dE} m_E \sin(\delta_E) V_{dc}) / (2x_{d\Sigma}) - \\ -(x_{dt} / x_{d\Sigma})(V_b \cos\delta + 0.5 m_B \sin(\delta_B) V_{dc}) \quad (30)$$

III. CONTROLLABILITY MEASURE

To measure the controllability of the EM mode by a given input (control signal), the singular value decomposition (SVD) is employed [17]. Mathematically, if G is a $m \times n$ complex matrix, then there exist unitary matrices U and V with dimensions of $m \times m$ and $n \times n$, respectively, such that:

$$G = U \Sigma V^H \quad (31)$$

where

$$\Sigma = \begin{bmatrix} \Sigma_1 & 0 \\ 0 & 0 \end{bmatrix}, \qquad \Sigma_1 = \operatorname{diag}(\sigma_1, ..., \sigma_r) \qquad \text{with}$$

$\sigma_1 \geq ... \geq \sigma_r \geq 0$ where $r = \min\{m, n\}$ and $\sigma_1, ..., \sigma_r$ are the singular values of G.

The minimum singular value σ_r represents the distance of the matrix G from all the matrices with a rank of $r-1$ [18]. This property can be used to quantify modal controllability [14, 15]. The matrix H can be written as $H = [h_1, h_2, h_3, h_4]$ where h_i is a column vector corresponding to the *i*th input.

The minimum singular value, $\sigma_{\min}$ of the matrix $[\lambda I - A, h_i]$ indicates the capability of the *i*th input to control the mode associated with the eigenvalue λ. Actually, the higher $\sigma_{\min}$, the higher the controllability of this mode by the input considered. As such, the controllability of the EM mode can be examined with all inputs in order to identify the most effective one to control the mode.

IV. DESIGN OF DAMPING CONTROLLERS

A. Conventional Lead-Lag Controller

The damping controllers are designed to produce an electrical torque in phase with the speed deviation. The four control parameters of the UPFC ($\Delta M_i, \Delta M_r, \Delta PH_i$ and ΔPH_r) can be modulated in order to produce the damping torque. The speed deviation is considered as the input to the damping controllers.

The structure of UPFC based damping controller is shown in Figure 3. It consists of gain, signal washout and phase compensator blocks. Figure 4 shows the block diagram of the system relating the electrical component of the power ΔP_{EM} produced by the damping controller δ_E.

The parameters of the damping controller are obtained using the phase compensation technique. The detailed step-by-step procedure for computing the parameters of the damping controllers using phase compensation technique is given below (for more details, readers can refer to [19]):

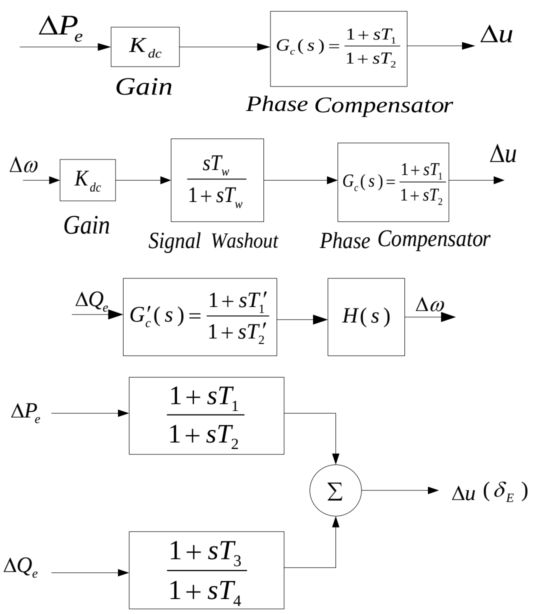

Figure 3. Structure of UPFC based damping controllers

1. Computation of natural frequency of oscillation ω_n from the mechanical loop.

$$\omega_n = \sqrt{\frac{K_1 \omega_0}{M}} \quad (32)$$

2. Computation of $\angle GEPA$ (K_c in [16]) at $s = j\omega_n$. Let it be γ.

3. Design of phase lead-lag compensator G_C:

The phase lead-lag compensator G_C is designed to provide the required degree of phase compensation. For 100% phase compensation,

$$\angle G_C(j\omega_n) + \angle GEPA(j\omega_n) = 0 \quad (33)$$

Assuming one lead-lag network, $T_1 = aT_2$ the transfer function of the phase compensator becomes,

$$G_C(s) = \frac{1+saT_2}{1+sT_2} \quad (34)$$

Since the phase angle compensated by the lead-lag network is equal to $-\gamma$, the parameters a and T_2 are computed as,

$$a = \frac{1+\sin(\gamma)}{1-\sin(\gamma)},\ T_2 = \frac{1}{\omega_n \sqrt{a}} \quad (35)$$

4. Computation of optimum gain K_{dc} for desired damping.

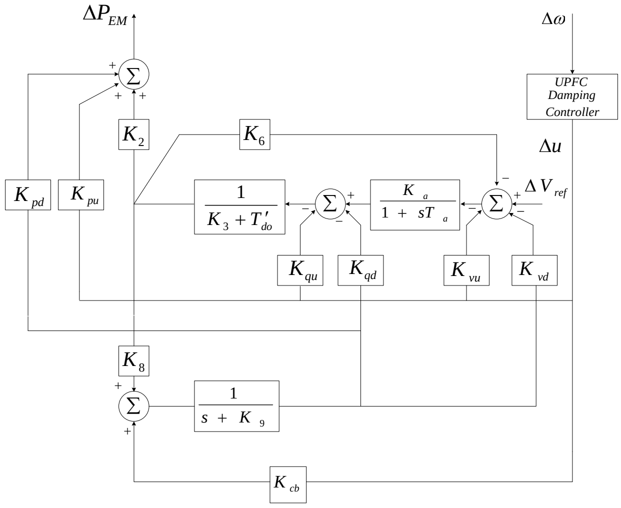

Figure 4. Block diagram of the system relating component of electrical power ΔP_{EM} produced by damping controller δ_E

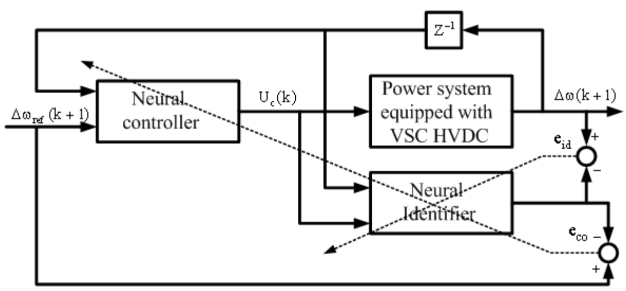

Figure 5. Structure of the online neural controller

B. Supplementary Damping Controller Based Adaptive Neural Network

The power system linearized model cannot be appropriate during the severe disturbances like the faults. Also, designed controllers based this model may be had unacceptable response in nonlinear power system model. So in this paper an adaptive neural controller is proposed to use in nonlinear model as shown in Figure 5. This adaptive neural controller is consisted from two separate neural networks as identifier and controller described in following.

C. Neural Identifier

Structure of neural identifier is shown in Figure 6. This network has four neuron at hidden and one at output layer. f is activation function that is hyperbolic tangent in this paper. It is trained using error back propagation method that described in detail in following.

Cost function is defined as:

$$E_{id} = \frac{1}{2}(\Delta\omega - \Delta\hat{\omega})^2 = \frac{1}{2}e_{id}^{\ 2} \quad (36)$$

$\Delta\omega$ and $\Delta\hat{\omega}$ are power system (i.e. rotor speed deviation) and neural identifier output, respectively.

$$\frac{\partial E_{id}}{\partial(\Delta\hat{\omega})} = -(\Delta\omega - \Delta\hat{\omega}) = -e_{id} \quad (37)$$

$$\frac{\partial E_{id}}{\partial w_{oh}^{id}} = \frac{\partial E_{id}}{\partial e_{id}} \frac{\partial e_{id}}{\partial(\Delta\hat{\omega})} \frac{\partial(\Delta\hat{\omega})}{\partial v} \frac{\partial v}{\partial w_{oh}^{id}} \quad (38)$$

where w_{oh}^{id} is weights between output and hidden layer. Using Equation (38), the sensitive coefficient of output neuron is calculated and output weights are updated according Equation (39).

$$w_{oh,New}^{id} = w_{oh,Old}^{id} - \eta \frac{\partial E_{id}}{\partial w_{oh}^{id}} \quad (39)$$

Using sensitive coefficient in output neuron, it is possible to correct other weights between hidden and input layer.

D. Neural Controller

Structure of neural controller is shown in Figure 7. This is a feed forward network including four neuron at hidden and one neuron at output layer. Back propagation method used to train this network as described in following. Cost function to training this network is:

$$E_{co} = \frac{1}{2}(0 - \Delta\hat{\omega})^2 = \frac{1}{2}\Delta\hat{\omega}^{\,2} = \frac{1}{2}e_{co}^{\ 2} \quad (40)$$

$$\frac{\partial E_{co}}{\partial(\Delta\hat{\omega})} = \Delta\hat{\omega} = -e_{co} \quad (41)$$

$$\frac{\partial E_{co}}{\partial w_{oh}^{co}} = \frac{\partial E_{co}}{\partial e_{co}} \frac{\partial e_{co}}{\partial(\Delta\hat{\omega})} \frac{\partial(\Delta\hat{\omega})}{\partial v} \frac{\partial v}{\partial w_{oh}^{co}} \quad (42)$$

V and w_{oh}^{co} are the neural identifier output and the weights between output and hidden layer of neural controller, respectively.

$$v = \sum_h w_{oh}^{id}.y_h^{mi\_id}$$
$$y_h^{mi\_id} = f(\sum_i w_{hi}^{id}.y_i^{in\_id}) = f(u_h) \quad (43)$$

$y_i^{in\_id}$, $y_h^{mi\_id}$, w_{hi}^{id}, w_{oh}^{id}, i and h are inputs, inputs to output layer, connection weights between input and hidden layer, weights between output and hidden layer, number of inputs and number of neuron in hidden layer of neural identifier, respectively, where:

$$\frac{\partial v}{\partial w_{oh}^{co}} = \frac{\partial v}{\partial U_c}\frac{\partial U_c}{\partial w_{oh}^{co}} = \frac{\partial v}{\partial y_h^{mi\_id}}\frac{\partial y_h^{mi\_id}}{\partial U_c}\frac{\partial U_c}{\partial w_{oh}^{co}} \tag{44}$$

Using Equations (42)-(44), it is possible to calculate the sensitive coefficient in output neuron of neural controller and correct the middle and output weights of neural controller.

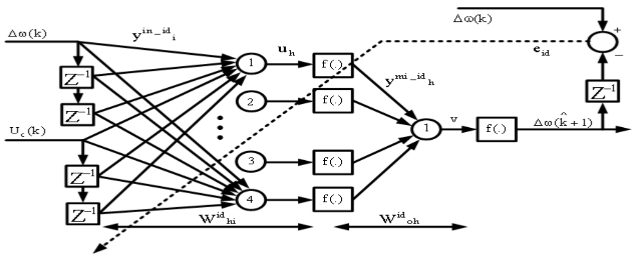

Figure 6. Structure of the online neural identifier

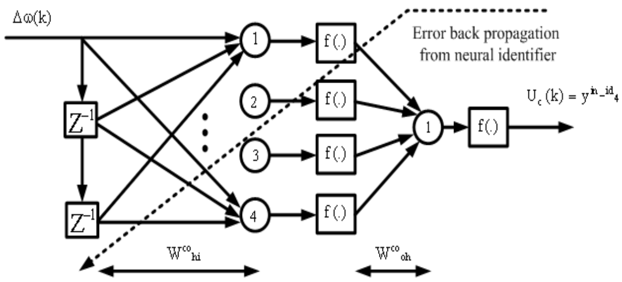

Figure 7. Structure of the online neural controller

V. SIMULATION RESULTS

Power system information is given in Appendix A. Constant coefficients in (7) are calculated according information which given in Appendix B. For given information, system poles are:

$-19.1186,\ 0.0122 \pm j4.0935,\ -1.2026$

It is clear that the uncompensated system is unstable.

A. Controllability Measure

SVD is employed to measure the controllability of the electromechanical mode (EM) mode from each of the four inputs: $m_B, \delta_E, m_E, \delta_B$. The minimum singular value $\sigma_{\min}$ is estimated over a wide range of operating conditions. For SVD analysis, P_e ranges from 0.01 to 1.5 pu and $Q_e = 0.4$ pu . At this loading condition, the system model is linearized, the EM mode is identified, and the SVD-based controllability measure is implemented. For comparison purposes, the minimum singular value for all inputs at $Q_e = 0.4$ pu is shown in Figure 8, respectively. From these figures, the following can be noticed:

- EM mode controllability via is δ_E always higher than that of any other input.
- The capabilities of δ_E and Δm_E to control the EM mode is higher than that of δ_B and Δm_B .
- The EM mode is controllable with δ_B than with Δm_B .

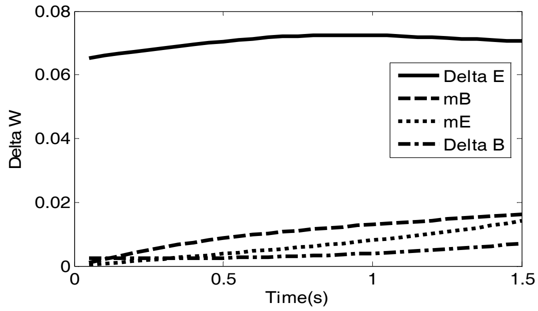

Figure 8. Controllability measure using singular value decomposition for oscillation mode

B. Results for Controllers Designed Based on SVD Results

At nominal load condition, the system without any controller's eigenvalues are given in section V. It is clear that the open loop system is unstable. According to SVD results, $\Delta\delta_E$ has a good controllability rather to others system inputs. So it is selected to apply supplementary control signal. Phase and neural controller's information are given in Appendix A.

C. Testing Proposed Supplementary Controllers

To assess the effectiveness of the proposed stabilizers two different operating conditions are considered according Table 1.

Table 1. Synchronous machine condition

Operating Condition	P_e	Q_e	V_t
λ_1 (Light)	0.2	0.1	1
λ_2 (Nominal)	0.8	0.167	1
λ_3 (Heavy)	1.2	0.4	1

The parameters of designed phase compensator are $T_1 = 0.2296$, $T_2 = 0.2516$, $K_{dc} = 18.0960$. This controller is designed for nominal operating condition. Neural networks weight are selected random from [0, 1]. Testing linear model consists of small changing in mechanical power ($\Delta P_m = 0.05$). Testing nonlinear model includes three phase fault at infinite bus at time $t = 1$ s that is removed after 5 cycles and changing in mechanical power ($\Delta P_m = 0.1$).

Figure 9 shows the linear power system response in condition λ_1 and λ_2 and λ_3, with phase compensator, respectively. According to this figure and with comparing them to Figure 10, neural network damps rotor speed oscillations better than phase compensator for small disturbances. In Figures 11-12 a three phase fault at $t = 1$ s accurse and clears after 5 cycles. It is considered that phase compensator cannot damp oscillations for large disturbances; however neural controller has a good response in all operating conditions. As a result, neural controller improves dynamical and transient stability, effectivenessly.

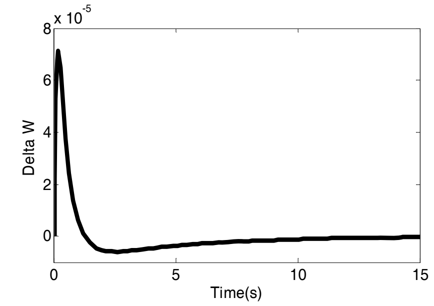

(a)

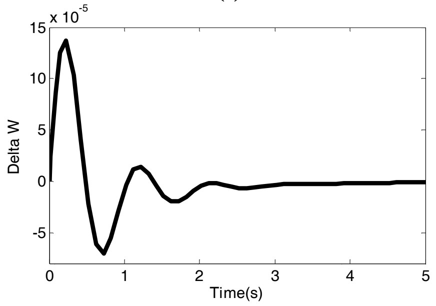

(b)

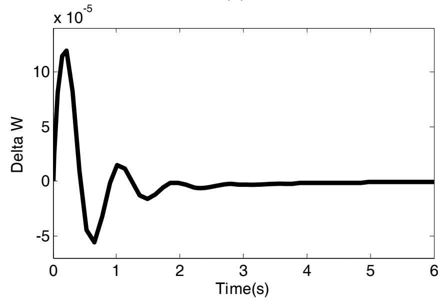

(c)

Figure 9. Dynamic responses of $\Delta\omega$ with input control signal δ_E and phase compensator for different operating conditions - Linear power system response in $\Delta P_m = 0.05$ with Phase compensator

(a): Light load (λ_1) (b): Nominal load (λ_2) (c): Heavy load (λ_3)

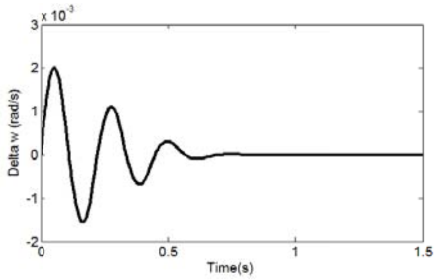

(a)

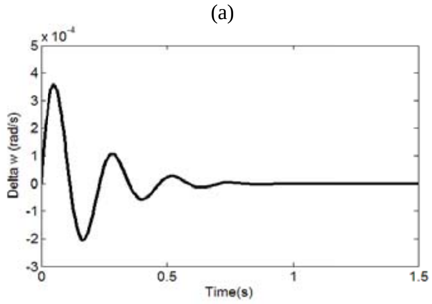

(b)

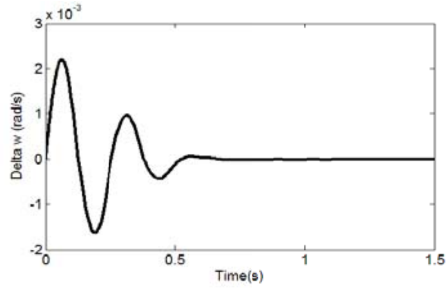

(c)

Figure 10. Dynamic responses of $\Delta\omega$ with input control signal δ_E Neural controller for different operating conditions - Nonlinear power system response in $\Delta P_m = 0.1$

(a): Light load (λ_1) (b): Nominal load (λ_2) (c): Heavy load (λ_3)

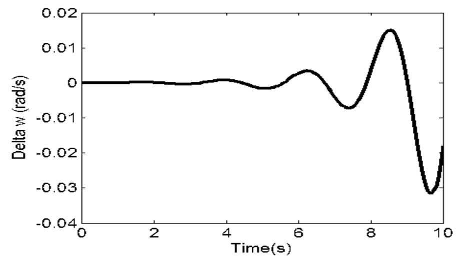

Figure 11. Rotor speed deviation - Nonlinear power system response in λ_2 and three phase fault in infinite bus with Phase compensator

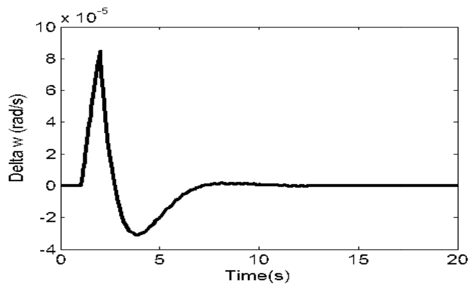

Figure 12. Rotor speed deviation - Nonlinear power system response in λ_2 and three phase fault in infinite bus with Neural controller

VI. CONCLUSIONS

In this paper, a novel dynamic model is considered and supplementary controller is designed for improve power system stability and oscillation damping. SVD has been employed to evaluate the EM mode controllability to the four UPFC input. SVD illustrated that the EM mode has best controllability via the fire angle of rectifier. Also, for improving the system stability and damping oscillations, a neuro controller is proposed. The simulation results has been carried out by Matlab/Simulink show designed neural controller for system has the perfectly effect in dynamic and transient improvement in comparison with phase compensator.

APPENDICES

Appendix A

Neural controller: two multilayer feed forward neural network with activation function: $a\tanh(bx)$.

Hidden and output layer for identifier includes 4 and 1 neuron respectively with $a = b = 1,\ Eta = 0.1$.
Hidden and output layer for controller includes 3 and 1 neuron respectively with $a = 20,\ b = 0.9,\ Eta = 0.1$.

Appendix B
The test system parameters are:
Generator:
$M = 2H = 8.0$ MJ/MVA, $D = 0.0$, $T'_{do} = 5.044$ s
$X_d = 1.0$ pu, $X_q = 0.6$ pu, $X'_d = 0.3$ pu
Excitation System:
$K_a = 100$, $T_a = 0.01$ s
Transformer:
$X_{tE} = 0.1$ pu, $X_E = X_B = 0.1$ pu, $X_E = X_B = 0.1$ pu
Transmission Line:
$X_{BV} = 0.3$ pu, $X_e = X_{BV} + X_B + X_{tE} = 0.5$ pu
Operating Condition:
$V_t = 1.0$ pu, $P_e = 0.8$ pu, $V_b = 1.0$ pu, $f = 60$ Hz
Parameters of DC Link:
$V_{dc} = 2$ pu, $C_{dc} = 1$ pu

Appendix C
Coefficients are:

$$K_1 = \frac{(V_{td} - I_{tq}x'_d)(x_{dE} - x_{dt})V_b \sin\delta}{x_{d\Sigma}} + \frac{(x_q I_{td} + V_{tq})(x_{qt} - x_{qE})V_b \cos\delta}{x_{q\Sigma}}$$

$$K_2 = \frac{-(x_{BB} + x_E)V_{td}}{x_{d\Sigma}x_d} + \frac{(x_{BB} + x_E)x'_d I_{tq}}{x_{d\Sigma}}$$

$$K_3 = 1 + \frac{(x'_d - x_d)(x_{BB} + x_E)}{x_{d\Sigma}},\ K_4 = -\frac{(x'_d - x_d)(x_{dE} - x_{dt})V_b \sin\delta}{x_{d\Sigma}}$$

$$K_5 = \frac{V_{td}x_q(x_{qt} - x_{qE})V_b \cos\delta}{V_t x_{q\Sigma}} - \frac{V_{tq}x'_d(x_{dtE} - x_{dt})V_b \sin\delta}{V_t x_{d\Sigma}}$$

$$K_6 = \frac{V_{tq}(x_{d\Sigma} + x'_d(x_{BB} + x_E))}{V_t x_{d\Sigma}}$$

$$K_7 = 0.25C_{dc}(V_b \sin\delta(m_E \cos\delta_E x_{dE} - m_B \cos\delta_B x_{dt})) - -\frac{m_B \cos\delta_B x_{dt}}{x_{d\Sigma}} + V_b \cos\delta(m_B \sin\delta_B x_{qt} - m_E \sin\delta_E x_{qe}$$

$$K_8 = -0.25\frac{m_B \cos\delta_B x_E + m_E \cos\delta_E x_{BB}}{x_{d\Sigma}}$$

$$K_9 = 0.25C_{dc}(\frac{m_B \sin\delta_B(m_B \cos\delta_B x_{dt} - m_E \cos\delta_E x_{dE})}{2x_{d\Sigma}} + \frac{m_E \sin\delta_E(m_E \cos\delta_E x_{Bd} - m_B \cos\delta_B x_{dt})}{2x_{d\Sigma}} + \frac{m_B \cos\delta_B(m_B \sin\delta_B x_{qt} - m_E \sin\delta_E x_{qE})}{2x_{q\Sigma}} + \frac{m_E \cos\delta_E(-m_B \sin\delta_B x_{qE} + m_E \sin\delta_E x_{Bq})}{2x_{q\Sigma}})$$

$$K_{pe} = \frac{(V_{td} - I_{tq}x'_d)(x_{Bd} - x_{dE})V_{dc}\sin\delta_E}{2x_{d\Sigma}} + \frac{(x_q I_{td} + V_{tq})(x_{Bq} - x_{qE})V_{dc}\cos\delta_E}{2x_{q\Sigma}}$$

$$K_{p\delta E} = \frac{(V_{td} - I_{tq}x'_d)(x_{Bd} - x_{dE})V_{dc}m_E\cos\delta_E}{2x_{d\Sigma}} + \frac{(x_q I_{td} + V_{tq})(-x_{Bq} + x_{qE})V_{dc}m_E\sin\delta_E}{2x_{q\Sigma}}$$

$$K_{pb} = \frac{(V_{td} - I_{tq}x'_d)(x_{dt} - x_{dE})x_{dc}\sin\delta_B}{2x_{d\Sigma}} + \frac{(x_q I_{td} + V_{tq})(x_{qt} - x_{qE})V_{dc}\cos\delta_B}{2x_{q\Sigma}}$$

$$K_{p\delta B} = \frac{(V_{td} - I_{tq}x'_d)(x_{dE} + x_{dt})V_{dc}m_B\cos\delta_B}{2x_{d\Sigma}} + \frac{(x_q I_{td} + V_{tq})(-x_{qt} + x_{qE})V_{dc}m_B\sin\delta_B}{2x_{q\Sigma}}$$

$$K_{pd} = (V_{td} - I_{tq}x'_d)(\frac{(x_{dt} - x_{dE})m_B\sin\delta_B}{2x_{d\Sigma}} + \frac{(x_{Bd} - x_{dE})m_E\sin\delta_E}{2x_{d\Sigma}}) + +(x_q I_{td} + V_{tq})(\frac{(x_{qt} - x_{qE})m_B\cos\delta_B}{2x_{q\Sigma}} + \frac{(x_{Bq} - x_{qE})m_E\cos\delta_E}{2x_{q\Sigma}}$$

$$K_{qe} = -\frac{(x'_d - x_d)(x_{Bd} - x_{dE})V_{dc}\sin\delta_E}{2x_{d\Sigma}}$$

$$K_{q\delta e} = -\frac{(x'_d - x_d)(x_{Bd} - x_{dE})m_E V_{dc}\cos\delta_E}{2x_{d\Sigma}}$$

$$K_{qb} = -\frac{(x'_d - x_d)(x_{dt} - x_{dE})V_{dc}\sin\delta_B}{2x_{d\Sigma}}$$

$$K_{q\delta B} = -\frac{(x'_d - x_d)(x_{dE} - x_{dt})m_B V_{dc}\cos\delta_B}{2x_{\Sigma}}$$

$$K_{qe} = -(x'_d - x_d)(\frac{(x_{Bd} - x_{dE})m_E\sin\delta_E}{2x_{d\Sigma}} + \frac{(x_{dt} - x_{dE})m_B\sin\delta_B}{2x_{d\Sigma}})$$

$$K_{ve} = \frac{V_{td}(x_{Bq} - x_{qE})V_{dc}\cos\delta_E}{2V_t x_{q\Sigma}} - \frac{V_{tq}(x_{Bd} - x_{dE})V_{dc}\sin\delta_E}{2V_t x_{d\Sigma}}$$

$$K_{v\delta E} = \frac{V_{td}x_q(x_{qE} - x_{Bq})m_E V_{dc}\sin\delta_E}{2V_t x_{q\Sigma}} - \frac{V_{tq}x'_d(x_{Bd} - x_{dE})m_E V_{dc}\cos\delta_E}{2V_t x_{q\Sigma}}$$

$$K_{vb} = \frac{V_{td} x_q (x_{qt} - x_{qE}) V_{dc} \cos\delta_E}{2V_t x_{q\Sigma}} - \frac{V_{tq} x'_d (x_{dt} - x_{dE}) V_{dc} \sin\delta_E}{2V_t x_{d\Sigma}}$$

$$K_{v\delta B} = \frac{V_{td} x_q (x_{qE} - x_{qt}) m_B V_{dc} \sin\delta_E}{2V_t x_{q\Sigma}} + \frac{V_{tq} m_B x'_d (x_{dE} + x_{dt}) V_{dc} \cos\delta_E}{2V_t x_{d\Sigma}}$$

$$K_{vd} = \frac{V_{td} x_q (x_{Bq} - x_{qE}) m_E \cos\delta_E}{2V_t x_{q\Sigma}} + \frac{(x_{qt} - x_{qE}) m_B \cos\delta_B}{2x_{q\Sigma}} - \frac{V_{tq} m_E x'_d (x_{Bd} - x_{dE}) \sin\delta_E}{2V_t x_{d\Sigma}} + \frac{m_B (x_{dt} - x_{qE}) \sin\delta_E}{2x_{d\Sigma}}$$

$$K_{ce} = 0.25C_{dc} \frac{V_{dc} \sin\delta_E (m_E \cos\delta_E x_{Bd} - m_B \cos\delta_B x_{dE})}{2x_{d\Sigma}} + \frac{V_{dc} \cos\delta_E (m_E \sin\delta_E x_{Bq} - m_B \sin\delta_B x_{qE})}{2x_{q\Sigma}}$$

$$K_{c\delta e} = \frac{0.25 m_E}{C_{dc}} (\cos\delta_E I_{Eq} - \sin\delta_E I_{Ed}) + \frac{0.25}{C_{dc}} (m_E V_{dc} \cos\delta_E \frac{(m_E \cos\delta_E x_{Bd} - m_B \cos\delta_B x_{dE})}{2x_{d\Sigma}} + m_E V_{dc} \sin\delta_E \frac{(m_B \sin\delta_B x_{qE} + m_E \sin\delta_E x_{Bq})}{2x_{q\Sigma}})$$

$$K_{cb} = 0.25C_{dc} \frac{V_{dc} \sin\delta_B (-m_E \cos\delta_E x_{dE} + m_B \cos\delta_B x_{dt})}{2x_{d\Sigma}} + \frac{V_{dc} \cos\delta_B (m_B \sin\delta_E x_{qt} - m_E \sin\delta_E x_{qE})}{2x_{q\Sigma}}$$

$$K_{c\delta B} = \frac{0.25 m_B}{C_{dc}} (\cos\delta_B I_{Bq} - \sin\delta_B I_{Bd}) + \frac{0.25}{C_{dc}} (m_B V_{dc} \cos\delta_B \frac{(m_E \cos\delta_E x_{dE} + m_B \cos\delta_B x_{dt})}{2x_{d\Sigma}} + m_B V_{dc} \sin\delta_B \frac{(-m_B \sin\delta_E x_{qt} + m_E \sin\delta_E x_{qE})}{2x_{q\Sigma}})$$

ACKNOWLEDGEMENTS

This work was supported by the SAMA Technical and Vocational Training College, Islamic Azad University, Kermanshah Branch, Kermanshah, Iran.

REFERENCES

[1] A.T. Al-Awami, Y.L. Abdel-Magid, M.A. Abido, "A Particle-Swarm-Based Approach of Power System Stability Enhancement with Unified Power Flow Controller", Elsevier, Electrical Power and Energy Systems, Vol. 29, No. 3, pp. 251-259, 2007.

[2] D.K. Chaturvedi, O.P. Malik, P.K. Kalra, "Performance of a Generalized Neuron Based PSS in a Multimachine Power System", IEEE Trans., 0885-8969/04$20.00, 2004.

[3] H.F. Wang, F.J. Swift, "A Unified Model for the Analysis of FACTS Devices in Damping Power System Oscillations - Part I: Single-machine Infinite-Bus Power Systems", IEEE Trans. Power Delivery, Vol. 12, No. 2, pp. 941-946, 1997.

[4] N. Yang, Q. Liu, J.D. McCalley, "TCSC Controller Design for Damping Interarea Oscillations", IEEE Trans. on Power Systems, Vol. 13, No. 4, pp. 1304-1310, 1998.

[5] E. Uzunovic, C.A. Canizares, J. Reeve, "EMTP Studies of UPFC Power Oscillation Damping", Proc. of NAPS'99, pp. 155-163, California, 1999.

[6] M. Villablanca, J. del Valle, J. Rojas, J. Abarca, W. Rojas, "A Modified Back-to-Back HVDC System for 36-Pulse Operation", IEEE Trans., Vol. 15, No. 2, 2000.

[7] H.R. Najafi, F. Robinson, A. Shoulaie, "Low Frequency Oscillation Analysis in Parallel AC/DC System by a Novel Dynamic Model", Powercon 2004, Vol. 1, pp. 294-99, 2004.

[8] A. Hammad, C. Taylor, "HVDC Controllers for System Dynamic Performance", IEEE Trans. on Power System, Vo1. 6, No. 2, pp. 743-752, 1991.

[9] J.O. Gjerdc, R. Flolo, T. Gjengeddal, "Use of HVDC and FACTS Components for Enhancement of Power System Stability", 8th Mediterranean Electro Technical Conf., MELECON 96, Vol. 2, pp. 802-808, 1996.

[10] G.M. Huang, V. Krishnaswamy, "HVDC Controls for Power System Stability", IEEE Power Eng. Society Summer Meeting, Vol. 1, pp. 597-602, 2002.

[11] M. Baker, K. Abbott, B. Gemmell, "Frequency and System Damping Assistance from HVDC and FACTS Controller", IEEE Power Engineering Society Summer Meeting, Vol. 2, pp. 770-773, 2002.

[12] S. Corsi, et al, "Emergency Stability Controls through HVDC Links", IEEE Power Eng. Society Summer Meeting, Vol. 2, pp. 774-779, 2002.

[13] P. Shamsollahi, O.P. Malik, "Direct Neural Adaptive Control Applied to Synchronous Generator", IEEE Trans. on Energy Conversion, Vol. 14, No. 4, pp. 1341-1346, 1999.

[14] P. Shamsollahi, O.P. Malik, "Application of Neural Adaptive Power System Stabilizer in a Multi-Machine Power System", IEEE Trans. on Energy Conversion, Vol. 14, No. 3, pp. 731-736, 1999.

[15] P. Shamsollahi, O.P. Malik, "Real-Time Implementation and Experimental Studies of a Neural Adaptive Power System Stabilizer", IEEE Trans. on Energy Conversion, Vol. 14, pp. 737-742, 1999.

[16] W. Liu, G. Venayagamoorthy, D. Wunsch, "Adaptive Neural Network Based Power System Stabilizer Design", IEEE International Joint Conference on Neural Networks, Vol. 4, pp. 2970-2975, July 2003.

[17] A.M.A. Hamdan "An Investigation of the Significance of Singular Value Decomposition in Power System Dynamics", Elsevier Elect. Power Energ. Sys., pp. 417-424, 1999.

[18] N.M. Tabatabaei, A. Hashemi, N. Taheri, F.M. Sadikoglu, "A Novel Online Adaptive Based Stabilizer for Dynamic Stability Improvement with UPFC", International Journal on Technical and Physical Problems

of Engineering (IJTPE), Issue 8, Vol. 3, No. 3, pp. 93-99, September 2011.
[19] N.M. Tabatabaei, A. Demiroren, N. Taheri, A. Hashemi, N.S. Boushehri, "SVD-UPFC Based Designation of Versatile Controllers to Damp Low Frequency Oscillations", International Journal on Technical and Physical Problems of Engineering (IJTPE), Issue 9, Vol. 3, No. 4, pp. 59-67, December 2011.

BIOGRAPHIES

Ahmad Hashemi was born in Kermanshah, Iran, in 1984. He received his B.Sc. degree in Power Electrical engineering from K.N. Toosi University of Technology, Tehran, Iran, in 2006 and his M.Sc. degree from Azarbaijan University of Tarbiat Moallem, Tabriz, Iran, in 2009. He is a member of Power Electrical Engineering Department at SAMA Technical and Vocational Training College, Islamic Azad University, Kermanshah Branch. Kermanshah, Iran. His main research interests are FACTS devices modeling, adaptive control and neural network optimizations.

Naser Mahdavi Tabatabaei was born in Tehran, Iran, 1967. He received the B.Sc. and the M.Sc. degrees from University of Tabriz (Tabriz, Iran) and the Ph.D. degree from Iran University of Science and Technology (Tehran, Iran), all in Power Electrical Engineering, in 1989, 1992, and 1997, respectively. Currently, he is a Professor of Power Electrical Engineering at International Organization of IOTPE (www.iotpe.com). He is also an academic board member of Power Electrical Engineering at Seraj Higher Education Institute (Tabriz, Iran) and teaches power system analysis, power system operation, and reactive power control. He is the secretary of International Conference of ICTPE, editor-in-chief of International Journal of IJTPE and chairman of International Enterprise of IETPE all supported by IOTPE. His research interests are in the area of power quality, energy management systems, ICT in power engineering and virtual e-learning educational systems. He is a member of the Iranian Association of Electrical and Electronic Engineers (IAEEE). He published more than 120 papers in international conferences and journals, 5 books, 8 conference proceedings and 11 journal issues.

Naser Taheri received the B.Sc. degree in Electronic Engineering from University of Guilan Rasht, Iran in 2007 and M.Sc. degree in Power Electrical Engineering from Azarbaijan University of Tarbiat Moallem, Tabriz, Iran in 2009. He is currently researching on power system control, flexible AC transmission systems (FACTS) and power systems dynamic modeling.

Saman Naderi was born in Kermanshah, Iran, on August 2, 1983. He received the B.Sc. degree in Electrical Engineering, 2007. His research interest is FACTS devices.